IEEE Access
Multidisciplinary ⋮ Rapid Review ⋮ Open Access Journal

Received January 19, 2021, accepted February 16, 2021, date of publication February 24, 2021, date of current version April 7, 2021.

Digital Object Identifier 10.1109/ACCESS.2021.3062026

Reliability Analysis for the Dependent Competing Failure With Wear Model and Its Application to the Turbine and Worm System

HAO LYU[1,2], XIAOWEN ZHANG[1], ZAIYOU YANG[1], SHUAI WANG[1], CHANGYOU LI[1], AND MICHAEL PECHT[2], (Life Fellow, IEEE)

[1]Mechanical Engineering and Automation, Northeastern University, Shenyang 110003, China
[2]Center for Advanced Life Cycle Engineering (CALCE), University of Maryland, College Park, MD 20742, USA

Corresponding author: Hao Lyu (haolyu@umd.edu)

This work was supported in part by the National Natural Science Foundation of China Project under Grant 51605083, in part by the fundamental research funds for the Central Universities of China Project under Grant N180304022, and in part by the China Scholarship Council Visiting Scholars Project under Grant 201906085037.

ABSTRACT Many systems are usually subjected to the combined effects of degradation and random shocks at the same time. Their failures are the competitive result of soft failure caused by degradation and hard failure caused by shocks. For operating machinery, wear failure is the main failure mechanism, and the machine is also subject to shock during the wear process. This paper proposes a new generalized surface wear model in combination with dependent competing failure processes; this proposed model is different from the other wear model with independent wear increments. As a typical mechanical structure, worm gears and worms are subjected to the combined effect of two failure mechanisms: soft failure caused by performance degradation, and hard failure caused by shocks. Meanwhile, it is necessary to consider the competitiveness and correlation of these two failure mechanisms. The interdependent competitive failure model is used to describe the failure of operating machinery. In this study, the extended Archard model is used to calculate the wear depth of the tooth surface, and the wear model is established through the wear threshold. The relationship between tooth surface wear depth and duty cycle, sliding speed, and contact stress is analyzed. An iterative algorithm is used to derive a nonlinear time-varying wear degradation model considering contact stress and sliding velocity. Comparing the calculation results with the Monte Carlo simulation method, the model has high accuracy and describes the mechanism of soft and hard failures, and the mutual dependence of the two failure mechanisms has an important effect on reliability. Numerical examples are presented to illustrate the developed reliability models, along with sensitivity analysis.

INDEX TERMS Archard model, dependent competing failure, hard failure threshold, system reliability, wear degradation.

I. INTRODUCTION

There are many kinds of modeling based on wear mechanisms, but there are many variables affecting wear; it is challenging to build a universal wear model for a particular mechanical component. The establishment of the wear model can be traced back to 1946. Holm [1] proposed a linear wear model that introduced the wear rate k on the basis of experiments, which made the theory consistent with the experimental results. Archard [2] perfected the linear model in 1953. This wear model considers the relationship between contact stress, slip velocity, and wear amount. This model is widely used in the establishment of adhesive wear models. Taking into acco-nt the nonlinearity in the degradation process will signifycan-tly improve the accuracy of the remaining useful life estimation [3]. Sharif *et al.* [4] predicted the wear pattern of worm gear teeth under lubrication conditions and determined the amount of wear calculation for each meshing cycle on the basis of full elastohydrodynamic lubrication. Ding and Kahraman [5] studied the nonlinear wear of spur gear transmission and the relationship between surface wear and dynamic behavior under nonlinear wear behavior. Based on Archard's law, Jbily *et al.* [6] combined contact pressure and sliding distance to determine the amount of wear, applying the law locally to calculate the wear depth of each contact point. Dorini [7] established a stochastic

The associate editor coordinating the review of this manuscript and approving it for publication was Nagarajan Raghavan.

model of the wear process using the Archard model based on the uncertainty of the wear coefficient related to the contact state. Fontanar *et al.* [8] studied the abrasion damage mechanism of bronze materials as the benchmark of worm gear power transmission. Through the lubrication rolling sliding experiment, the wear curve (specific gravity loss and sliding distance) and surface damage were analyzed using an optical microscope and scanning electron microscope. It was found that the severity of different types of wear damage depends on the applied load. Wang and Morrish [9] proposed a model for iteratively performing wear steps as needed. This model mainly considers the load distribution and contact stress of the worm gear during operation. Liu *et al.* [10] established the equation of the main factors influencing the wear of the tooth profile, such as relative sliding coefficient and contact compressive stress. In these wear models, the influence of parameters such as wear rate and contact stress on the degree of wear is studied, and the randomness of the parameters involved in the wear model is considered. In fact, in the normal working phase, the research object will inevitably be affected by external factors due to external environmental fluctuations, such as external shocks and unstable operating temperatures. Therefore, when establishing the wear model, external forces should also be taken into consideration as a factor that affects the degree of wear.

In general, many complex systems may gradually deteriorate due to wear, fatigue, corrosion, and other reasons. Due to excessive load, shock, and other pressures, the system may also suddenly fail. The former is called a soft failure, and the latter is called a hard failure [11]. For a system with multiple related competing risks, the total degradation includes the amount of natural degradation and the sudden increase in degradation caused by random shocks [12]. In practice, the relationship between soft failure and hard failure is interdependent; therefore, these processes are called dependent competitive failure processes (DCFPs) [13]. In recent years, many researchers have conducted reliability analyses on systems with dependent competitive failure processes, Competitive failure modeling methods have been extensively studied. Gao *et al.* [14] proposed reliability models for degradation-shock dependence systems with multiple species of shocks. In this research, he considered the correlation between soft failure and hard failure based on two different shock effect patterns (SEPs), namely degradation level and degradation rate, and developed four reliability models for different random processes and SEPs. Qiu and Cui [15] studied the optimal mission abort policy based on a two-stage Gamma process. He obtained the relationship between mission reliability and abort threshold, and the functional relationship between system survivability and mission abort threshold. Song *et al.* [16] developed a new multi-component system reliability model which extend component-level degradation modeling concepts to the system level. For the first time, Lin *et al.* [17] considered the reliability of the system under continuous and multi-state degradation processes, random shocks and their correlations, and proposed a reliability model for systems that experienced degradation processes and random shocks. In addition to reliability modelling, the condition based maintenance modelling is another research topic related to degradation modelling. For a series system with two non-identical units, Wang *et al.* [18] proposed a joint optimization problem of condition-based and age-based replacement strategy and spare parts inventory strategy

Many types of research are devoted to the reliability modeling of degraded processes and competitive failures under random shocks. Fan *et al.* [19] considered the shock system that is subjected to a nonuniform Poisson process. Degradation will affect the shock effect and increase the shock amplitude. Fan *et al.* [20] proposed a new reliability model of dependent competition failure, which considers that the strength of random shock depends on the degradation process. Rafiee *et al.* [21] considered four specific random shock modes that can increase the degradation rate. The study also pointed out through calculation examples that the micro-engine is more prone to wear degradation and accelerates the wear process when it is in a specific mode of shock or a significant shock. Gut and Hüsler [22] derived a generalized extreme shock model, assuming that nonfatal shocks may affect the system's resistance to subsequent shocks. Chatwattanasiri *et al.* [23] proposed a competitive failure reliability model for a k-out-of-n system. The model has a linear degradation path with a normal distribution degradation rate and a random shock process with a normal distribution shock load size and shock damage size. The competitive failure models they proposed all consider the interdependence between external random shocks and the degradation process and assume that the hard failure threshold is a constant. However, as the system continues to degenerate, the ability of the research object to resist external shocks should also be reduced. Therefore, the degradation-influenced hard fault threshold should also be regarded as a dependency in competitive failure modeling. An *et al.* [24] developed a reliability model for a complex system that experiences multiple dependent competing failure processes with shock loads above a certain level, where only the shock loads with magnitude above a certain level can lead to sudden degradation increments. Hao and Yang [25] proposed a competitive failure reliability model with changes in degradation rate and hard failure threshold, taking into account the influence of random shocks on the degradation process, degradation rate, and hard failure threshold. Jiang *et al.* [26] studied the two dependencies of the shock process and the hard failure threshold level. In the linear degradation and shock competition failure model of the micro engine established in [27], shocks can be categorized into three shock zones according to their magnitudes: safety zone, damage zone, and fatal zone. Lehmann [28] considered that failure is a competitive model of degradation and trauma and established a degradation-threshold-shock model (DTS model). The DCFP system he established takes into account the change of threshold, but most of the models are used in micro-electromechanical systems, and for simple mechanical

systems, such as gears, bearings, bolts, and other mechanical components, the study of the DCFP model is established by considering the changes in their working conditions.

To sum up, in this study, we are committed to introducing the Archard wear model into the competitive failure model, treating wear as degradation, rather than treating the degradation process as a Gamma process or a simple linear path, and the established competitive failure model is applied to mechanical structures other than MEMS.

The worm gear transmission mechanism is a special type of gear transmission mechanism that has the characteristics of a large power transmission ratio, a stable transmission, and self-locking capability. Therefore, it is widely used in the reduction mechanism of metallurgy, mining, lifting, and other mechanical equipment. Since the worm gear is usually made of a softer material than the worm, the worm wheel and worm gear transmission mechanism often suffer from the wear failure of the worm wheel. Excessive wear of the worm gear material will reduce the transmission accuracy and work efficiency and will also cause noise and vibration [29], [30]. At the same time, the backlash will increase the vibration amplitude of the tooth, the meshing force, and the shock behind the tooth [31]. In short, in the operation of the worm mechanism, there is sliding friction between the teeth resulting in excessive power loss, a reduction in gear efficiency, and even the failure of the mechanism. In order to optimize the wear conditions of the worm gear, a simple wear model is required. The wear prediction model proposed by Flodin and Andersson [32] takes into account the operating conditions of the gear tooth surface and uses the Winkler elastic foundation model to simulate contact between the tooth surfaces and simulate the tooth profile wear process. Kahraman *et al.* [33] proposed a gear wear model that combines a finite-element-based gear contact mechanics model to predict contact pressures; they also employed a sliding distance computation algorithm and Archard's wear formulation to predict wear of the contacting tooth surfaces. Yuksel and Kahraman [30] defined a dynamic gear tooth surface wear. The results of gear surface wear show model for geometric description of the deformation body of that the surface wear has a greater effect in the nonresonant speed range, and the decrease in the effect near the resonance peak is mainly due to the effect of tooth pitch. At present, there is no perfect method for quantitative calculation of worm gear wear. The worm gear is subjected to shock load during work, which causes the surface of the worm wheel to wear and produces debris, and the debris reacts to accelerate the wear of the worm wheel [34]. Metal particles are generated on the surface of the worm gear, and the metal particles enter the lubricating oil to accelerate the sliding wear of the worm gear teeth. At the same time, when the shock load exceeds a certain threshold, the mechanism will fail to lock itself. Therefore, the worm gear drive mechanism experiences two competing failure processes: worm gear wear and external shock, the combined action of which causes degradation of the mechanism. Performance degradation is regarded as a soft failure process, and failures caused by excessive shock loads are regarded as hard failures [35]. Based on the reliability modeling method combined with worm gear wear degradation analysis, the reliability modeling problem of worm gear can be solved.

Due to the uncertainty of the related parameters of worm gear wear, the current research on worm gears mainly focuses on wear model and life prediction, rather than reliability modeling. The reliability of worm gear is usually calculated by the contact strength of the tooth surface and the bending strength of the tooth root. Currently, the prognostic process development and parameter selections tend to focus on empirical results, experience, and maintenance data rather than on the physical processes that lead to failures [36]. Based on the Archard model, this paper combines contact stress and sliding speed to determine the wear of the worm gear tooth surface in the mine hoisting mechanism that needs a frequent start and stop capability. Combined with the wear model to analyze the reliability of the worm gear and worm, in the model wear is essentially a time-related degradation process, and the transmission mechanism is subjected to a time-independent shock process during work.

In summary, for the reliability modeling of worm gears, quantitative analysis of wear and the coupling relationship between wear and shock have not been considered. This paper combines the specific failure process of the worm gear of the mining machine's hoisting mechanism, introduces the dependence relationship into the failure mechanism model, and regards wear and shock as competing failure processes. The paper establishes the wear-shock coupling failure model and introduces the specific failure process of the worm gear in the lifting device of the mining machine.

The rest of the paper's structure is as follows: The second section discusses the dependence between wear degradation and shock and establishes a competitive failure model. The third section, based on Archard model, establishes the iterative time-varying wear calculation formula of running machinery with sliding wear. In the fourth section, combined with actual calculation examples, the first-order second-mom-ent method is used to establish the reliability model of the worm gear mechanism competition failure in the mine hoisting mechanism under random shock. In the fifth section, the Monte Carlo algorithm simulation is performed on the model under actual working conditions. The results show that the established model can describe the interdependent competitive failure behavior and interdependence relationship. And through sensitivity analysis, the influence of each parameter on the reliability of worm gear wear is discussed.

II. SYSTEM SPECIFICATION

The system's failure is the result of the combined effect of soft and hard failures, as shown in Fig. 1. In this paper, wear degradation failure is regarded as a soft failure. When the system's overall wear degradation performance exceeds the critical threshold level for the first time, a soft failure will occur, and random external shocks accelerate the degradation process. The hard failure threshold is affected by the

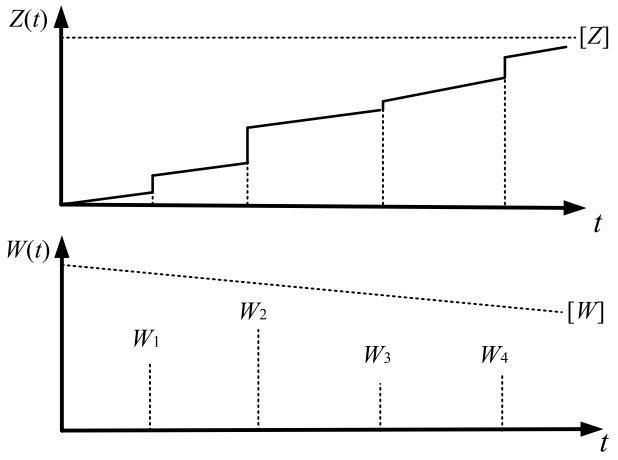

FIGURE 1. Competitive failure model.

total amount of degradation. Soft failure results from the cumulative damage caused by the combined action of wear degradation and random shock exceeding the threshold $[Z]$. Hao and Yang [25] proposed a competitive failure reliability model with threshold changes. In this model, the threshold level of the extended limit shock model will be reduced due to the harmful shock of the system, and every harmful shock will lead to a sudden increase in degraded performance; the coupling coefficient is introduced to establish the coupling relationship of the system. The overall description of the system and related expressions are as follows.

(1) In this paper, the wear process is regarded as a continuous degradation process, and the wear amount H(t) can be derived according to the Archard wear model.

(2) The shock is regarded as a homogeneous Poisson process with a constant velocity λ. The number of shocks arriving before time t is represented by $N(t)$.

$$p\left(N\left(t\right)=n\right)=\frac{e^{-(\lambda t)}\left(\lambda t\right)^{n}}{n!},\quad n=0,1,2\ldots \tag{1}$$

Each shock is independent of the other, normal pdf presents a normal behavior for a lot of random appearances [37], and the shock size follows the same normal distribution $W_i \sim N(\mu_{\mathrm{w}}, \sigma_{\mathrm{w}})$, where μ_{w} and σ_{w} are the average value and standard deviation of the shock size. W is the critical threshold level. When the shock size exceeds $[W]$, the system will have a hard failure.

(3) The continuous increase of wear degradation $Z(t)$ reduces the ability of equipment to resist harmful external shocks. The shock will be affected by the degradation process because the degradation process will affect the hard failure threshold $[W]$. When the degradation is $Z(t)$ at the system hard failure threshold level $[W]$, shown in eq. (2).

$$[W]=W_0+\gamma_W Z(t) \tag{2}$$

where W_0 is the initial hard failure threshold, and γ_W is the degradation conversion ratio coefficient.

(4) The degradation process is affected by random shocks. Each harmful shock leads to a sudden increase in wear degradation. The total degradation performance is affected, and the cumulative degree of harmful shocks reached is reflected. A coefficient γ_{h} is introduced to correct the amount of wear degradation.

$$Z(t)=H\left(t\right)+\gamma_h\sum W \tag{3}$$

where γ_{h} is the shock conversion ratio coefficient, $\sum W$ is the cumulative shock load.

(5) The threshold level of soft failure $[Z]$ is a constant; the threshold level can generally be calculated according to system parameters. If it involves the total degradation performance $Z(t)$ of the combined action of H(t) and W(t) exceeds $[Z]$, then the soft failure occurs immediately.

When the total amount of wear degradation is less than the failure threshold, taking into account the coupling relationship between wear degradation and the shock process, the wear degradation reliability $R_{\mathrm{Z}}(t)$ within the worm pair time t can be seen in eq. (4).

According to the extreme shock model and the coupling relationship between wear degradation and instantaneous shock, when i shocks occur within time t, the shock reliability $R_{\mathrm{W}}(t)$ of the worm pair can be seen in eq. (5).

$$\begin{aligned}R_{\mathrm{Z}}(t)&=P\left(Z\left(t\right)<[Z]\,|N\left(t\right)=i\right)P\left(N\left(t\right)=i\right)\\&=P\left(H\left(t\right)+\gamma_h\sum_{j=1}^{i}W_j<[Z]\,|N\left(t\right)=i\right)\\&\quad\times P\left(N\left(t\right)=i\right)\end{aligned} \tag{4}$$

$$\begin{aligned}R_{\mathrm{W}}(t)&=P\left(W_i<[W]\,|N\left(t\right)=i\right)P\left(N\left(t\right)=i\right)\\&=P\left(W_i<W_0+\gamma_w Z\left(t\right)|N\left(t\right)=i\right)P\left(N\left(t\right)=i\right)\end{aligned} \tag{5}$$

Then the reliability R of the worm pair in time t is shown in eq. (8).

$$R\left(t\right)=\sum_{i=1}^{\infty}P\left(Z\left(t\right)<[Z],W_i<[W]\,|N\left(t\right)=i\right)\cdot \times P\left(N\left(t\right)=i\right) \tag{6}$$

A. SYSTEM SOFT FAILURE RELIABILITY ANALYSIS

According to the derivation of the Archard model, the periodic function degenerate $h(t)=h(k_1(t), k_2(t),\ldots,p_1, p_2,\ldots)$ has multiple variables, where k is the probability of adhesive and the variable k_i is related to time. p is the contact stress, the variable p_i is a normal random variable, $p_i \sim N(\mu_i, \sigma_i)$, and i is a positive integer.

N(t) is used to denote the number of harmful shocks. $N(t)$ obeys the Poisson process of rate λ. Soft failure and hard failure are affected by the same shock process, and the effects of different numbers of shocks in the degradation process are considered. In the case of a fixed number of harmful shocks, wear reliability is derived in the following two situations.

(1) When the number of shocks $N(t)=i=0$, the calculation of reliability is shown in eq. (7), as shown at the bottom of the next page.

(2) When the number of shocks $N(t)=i>0$, the calculation of reliability is shown in eq. (8), as shown at the bottom of the next page.

B. SYSTEM HARD FAILURE RELIABILITY ANALISIS

Under a fixed number of shocks, the system reliability probability is as follows:

(1) When the number of shocks $N(t) = i = 0$, the calculation of reliability is shown in eq. (9), as shown at the bottom of the next page.

(2) When the number of shocks $N(t) = i > 0$, the calculation of reliability is shown in eq. (10), as shown at the bottom of the next page.

C. RELIABILITY ANALYSIS OF COMPETITIVE FAILURE PROCESS

The failure of a system is the result of competition between soft and hard failures. The conditional reliability functions of soft and hard failures are combined, and the reliability function of the overall system can be obtained as:

(1) When the number of shocks $N(t) = i = 0$, the calculation of reliability is shown in eq. (11), as shown at the bottom of the next page.

(2) When the number of shocks $N(t) = i > 0$, the calculation of reliability is shown in eq. (12), as shown at the bottom of the next page. eq. (12) can be applied to calculate mechanisms prone to sliding wear failure and shock failure. According to the actual working conditions and the specific research object, we can determine the relevant parameters and bring them into eq.(12) to calculate the reliability - time curve of the research object

III. WEAR DEGRADATION

Load, sliding speed, enhanced fracture toughness, contact surface morphology, and wear surface hardness are the significant parameters that affect material wear [38]. In the working process of the operating mechanism, wear always exists. The wear condition during a start-stop cycle is shown in Fig. 2.

In a start-stop cycle, the wear curves are mainly divided into three stages: running phase, normal wear phase, and the brake wear phase. The running phase is the wear during the motor's initial start. In this stage, the wear rate is relatively large due to the acceleration of the motor. In normal use, the mechanism will be subject to shock due to the influence of unfavorable factors, and a sudden change in the wear process will occur in the normal wear stage, resulting in severe wear. In the time t_a to time t_b in Fig. 2, the wear amount in this stage increases suddenly. When the wear exceeds the wear threshold, it will cause the research object to fail. This situation dramatically shortens the service life of the mechanism. Material wear thickness is affected by tooth surface stress and relative slip speed. Therefore, for a mechanism in normal operation, during a start-stop work cycle the wear amount is the largest in the start-stop phase.

A. WEAR ANALYSIS

In the Archard model [2], the wear depth of the research object is related to the sliding distance of the worm gear, the contact stress, and the yield strength of the material, as shown in eq. (13).

The left side of the formula is the wear depth h, and the right F/S is the nominal contact stress p. Therefore, the wear level can be measured by measuring the wear depth.

$$
\begin{aligned}
&R_s(t|N(t)=0) = P\{Z(t) < [Z]\,|N(t)=0\} \\
&= P\left\{\int_0^{t_1} h_1(k_1(\tau), k_2(\tau), k_3(\tau)\cdots, p_{11}, p_{12}, p_{13}\cdots)d\tau + \int_{t_1}^{t_2} h_2(k_1(\tau), k_2(\tau), k_3(\tau)\cdots, p_{21},\ p_{22}, p_{23}\cdots)\,d\tau + \cdots < [Z]\right\} \\
&\quad \times P\{N(t)=0\} \\
&= \Phi\left(\frac{[Z] - \int_0^{t_1} h_1(k_1(\tau), k_2(\tau)\cdots, \mu_1, \mu_2\cdots)d\tau - \int_{t_1}^{t_2} h_2(k_1(\tau), k_2(\tau)\cdots, \mu_1, \mu_2\cdots)d\tau - \cdots}{\sqrt{\sum_{i=1}^{N-1} m\left(k_1(t_i), k_2(t_i)\cdots, \sigma_1^2, \sigma_2^2\cdots\right) + m\left(k_1(t), k_2(t)\cdots, \sigma_1^2, \sigma_2^2\cdots\right)}}\right)\frac{(\lambda t)^0}{0!}e^{-\lambda t}
\end{aligned} \tag{7}
$$

$$
\begin{aligned}
&R_s(t|N(t)=i) = P\{Z(t) < [Z]\,|N(t)=i\} \\
&= P\left\{\int_0^{t_1} h_1(k_1(\tau), k_2(\tau), k_3(\tau)\cdots, p_{11}, p_{12}, p_{13}\cdots)d\tau + \int_{t_1}^{t_2} h_2(k_1(\tau), k_2(\tau), k_3(\tau)\cdots, p_{21},\ p_{22}, p_{23}\cdots)\,d\tau + \cdots\right. \\
&\quad \left. + \gamma_h \sum_{j=1}^{i} W_i < [Z]\right\} \cdot P\{N(t)=i\} \\
&= \Phi\left(\frac{[Z] - \int_0^{t_1} h_1(k_1(\tau), k_2(\tau)\cdots, \mu_1, \mu_2\cdots)d\tau - \int_{t_1}^{t_2} h_2(k_1(\tau), k_2(\tau)\cdots, \mu_1, \mu_2\cdots)\,d\tau - \cdots - i\gamma_h\mu_w}{\sqrt{\sum_{i=1}^{N-1} m\left(k_1(t_i), k_2(t_i)\cdots, \sigma_1^2, \sigma_2^2\cdots\right) + m\left(k_1(t), k_2(t)\cdots, \sigma_1^2, \sigma_2^2\cdots\right) + i\gamma_h\sigma_w^2}}\right)\frac{(\lambda t)^i}{i!}e^{-\lambda t}
\end{aligned} \tag{8}
$$

Since the research object's sliding speed generally changes with time during the working process, the contact stress may change. When the research object material is determined, the integral relationship between speed and time is introduced.

$$W = \frac{kdF}{3\sigma_s} \tag{13}$$

$$R_h\left(t|N(t)=0\right) = P\left\{0 < [W]\,|N(t)=0\right\} = P\left\{N(t)=0\right\} = \frac{(\lambda t)^0}{0!}e^{-\lambda t} \tag{9}$$

$$\begin{aligned}
&R_h\left(t|N(t)=i\right) = P\left\{W_i < [W]\,|N(t)=i\right\} \\
&= P\left\{W_i < W_0 + \gamma_{\mathrm{w}}\left[\int_0^{t_1} h_1(k_1(\tau), k_2(\tau), k_3(\tau)\cdots, p_{11}, p_{12}, p_{13}\cdots)d\tau\right.\right. \\
&\quad \left.\left. + \int_{t_1}^{t_2} h_2\left(k_1(\tau), k_2(\tau), \quad \cdots, p_{21}, p_{22}, \cdots\right)d\tau + \cdots + \gamma_{\mathrm{h}}\sum_{j=1}^{i-1} W_i\right]\right\} \cdot P\left\{N(t)=i\right\} \\
&= \Phi\left(\frac{W_0 + \gamma_{\mathrm{w}}\left(\int_0^{t_1} h_1(k_1(\tau), k_2(\tau)\cdots, \mu_1, \mu_2\cdots)d\tau + \int_{t_1}^{t_2} h_2\left(k_1(\tau), k_2(\tau)\cdots, \mu_1, \mu_2\cdots\right)d\tau + (i-1)\,\gamma_{\mathrm{h}}\mu_{\mathrm{w}}\right)\cdots - \mu_{\mathrm{w}}}{\sqrt{\sigma_{\mathrm{w}}^2 - \gamma_{\mathrm{w}}\left(\sum_{i=1}^{N-1} m\left(k_1(t_i), k_2(t_i)\cdots, \sigma_1^2, \sigma_2^2\cdots\right) + m\left(k_1(t), k_2(t)\cdots, \sigma_1^2, \sigma_2^2\cdots(i-1)\,\gamma_{\mathrm{h}}\sigma_{\mathrm{w}}^2\right)\right)}}\right) \\
&\quad \times \frac{(\lambda t)^i}{i!}e^{-\lambda t}
\end{aligned} \tag{10}$$

$$\begin{aligned}
&R\left(t|N(t)=0\right) = P\left\{Z(t) < [Z], 0 < [W]\,|N(t)=0\right\} \\
&= P\left\{\int_0^{t_1} h_1(k_1(\tau), k_2(\tau), k_3(\tau)\cdots, p_{11}, p_{12}, p_{13}\cdots)d\tau + \int_{t_1}^{t_2} h_2\left(k_1(\tau), k_2(\tau)\cdots, p_{21}, \quad p_{22}\cdots\right)d\tau + \cdots < [Z]\right\} P\left\{N(t)=0\right\} \\
&= \Phi\left(\frac{[Z] - \int_0^{t_1} h_1(k_1(\tau), k_2(\tau)\cdots, \mu_1, \mu_2\cdots)d\tau - \int_{t_1}^{t_2} h_2\left(k_1(\tau), k_2(\tau)\cdots, \mu_1, \mu_2\cdots\right)d\tau - \cdots}{\sqrt{\sum_{i=1}^{N-1} m\left(k_1(t_i), k_2(t_i)\cdots, \sigma_1^2, \sigma_2^2\cdots\right) + m\left(k_1(t), k_2(t)\cdots, \sigma_1^2, \sigma_2^2\cdots\right)}}\right)\frac{(\lambda t)^0}{0!}e^{-\lambda t}
\end{aligned} \tag{11}$$

$$\begin{aligned}
&R\left(t|N(t)=i\right) = P\left\{Z(t) < [Z], W_i < [W]\,|N(t)=i\right\} \\
&= P\left\{\int_0^{t_1} h_1(k_1(\tau), k_2(\tau), k_3(\tau)\cdots, p_{11}, p_{12}, p_{13}\cdots)d\tau + \int_{t_1}^{t_2} h_2\left(k_1(\tau), k_2(\tau), k_3(\tau)\cdots, \quad p_{21}, p_{22}, p_{23}\cdots\right)d\tau + \cdots\right. \\
&\quad + \gamma_{\mathrm{h}}\sum_{j=1}^{i} W_i < [Z], W_i < W_0 + \gamma_{\mathrm{w}}\left[\int_0^{t_1} h_1(k_1(\tau), k_2(\tau), k_3(\tau)\cdots, p_{11}, p_{12}, p_{13}\cdots)d\tau\right. \\
&\quad \left.\left. + \int_{t_1}^{t_2} h_2\left(k_1(\tau), k_2(\tau), k_3(\tau)\cdots, p_{21}, p_{22}, p_{23}\cdots\right)d\tau + \cdots + \gamma_{\mathrm{h}}\sum_{j=1}^{i-1} W_i\right]\right\} P\left\{N(t)=i\right\} \\
&= \Phi\left(\frac{[Z] - \int_0^{t_1} h_1(k_1(\tau), k_2(\tau)\cdots, \mu_1, \mu_2\cdots)d\tau - \int_{t_1}^{t_2} h_2\left(k_1(\tau), k_2(\tau)\cdots, \mu_1, \mu_2\cdots\right)d\tau - \cdots - i\gamma_{\mathrm{h}}\mu_{\mathrm{w}}}{\sqrt{\sum_{i=1}^{N-1} m\left(k_1(t_i), k_2(t_i)\cdots, \sigma_1^2, \sigma_2^2\cdots\right) + m\left(k_1(t), k_2(t)\cdots, \sigma_1^2, \sigma_2^2\cdots\right) + i\gamma_{\mathrm{h}}\sigma_{\mathrm{w}}^2}}\right) \cdot \\
&\quad \times \Phi\left(\frac{W_0 + \gamma_{\mathrm{w}}\left(\int_0^{t_1} h_1(k_1(\tau), k_2(\tau)\cdots, \mu_1, \mu_2\cdots)d\tau + \int_{t_1}^{t_2} h_2\left(k_1(\tau), \, k_2(\tau)\cdots, \mu_1, \mu_2\cdots\right)d\tau \cdots + (i-1)\,\gamma_{\mathrm{h}}\mu_{\mathrm{w}}\right) - \mu_{\mathrm{w}}}{\sqrt{\sigma_{\mathrm{w}}^2 - \gamma_{\mathrm{w}}\left(\sum_{i=1}^{N-1} m\left(k_1(t_i), k_2(t_i)\cdots, \sigma_1^2, \, \sigma_2^2\cdots\right) + m\left(k_1(t)\,, k_2(t)\cdots, \sigma_1^2, \sigma_2^2\cdots\right) + (i-1)\,\gamma_{\mathrm{h}}\sigma_{\mathrm{w}}^2}}\right) \\
&\quad \times \frac{(\lambda t)^i}{i!}e^{-\lambda t}
\end{aligned} \tag{12}$$

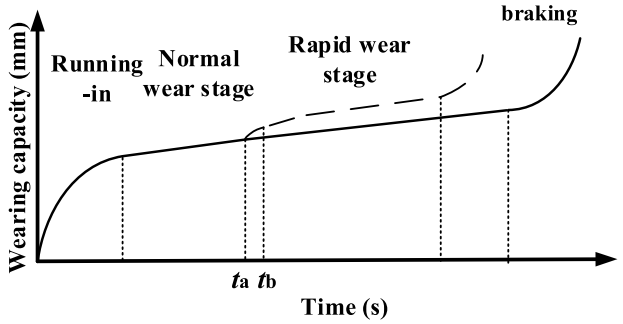

FIGURE 2. Sliding wear curve.

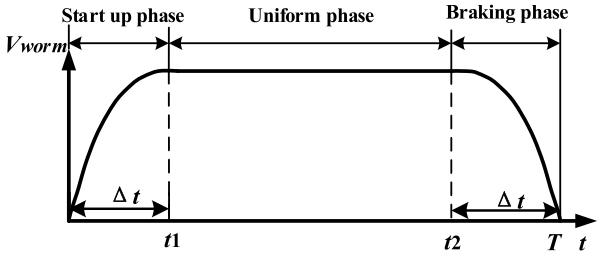

FIGURE 3. Speed curve of the rotating mechanism.

where W is the volume of wear material, d is the sliding distance and F is the applied load. k is the probability of adhesive wear; it is related to the low hardness of the research object's mating materials. σ_s is the yield strength of the material.

$$h = h(v(t), p(t), \sigma_s, k) = \int \frac{kp(t)v(t)}{3\sigma_s} dt \tag{14}$$

where $v(t)$ is the sliding velocity and $p(t)$ is the contact stress, which are all time-related variables.

1) CONTACT STRESS CALCULATION

Upon determination of the contact surface material where sliding wear occurs, the wear depth is only related to the sliding speed v and the contact stress p. The contact stress is related to the working load of the worm gear. Under stable working conditions, when the working load is determined the contact stress p is also a constant. When the working load is a normal random variable, the calculated nominal contact stress p_i should also be subject to the normal distribution; the mean value μ_p is the rated load

$$p_i \sim N\left(\mu_p, \sigma_p^2\right) \tag{15}$$

2) SLIDING SPEED DETERMINATION

The terminal load of the running machinery with sliding wear occurs in a start-stop cycle. The speed V is divided into three stages: acceleration, constant speed, and deceleration [39], and the given velocity curve is mainly uses the trapezoidal line chart [40]. The preset worm rotation speed curve in a working cycle is shown in Fig. 3.

The formula used to calculate the angular velocity of the motor starting phase is assumed to be:

$$\omega = \omega_0 \left(1 - e^{-t/\tau}\right) \tag{16}$$

where ω is the average working speed of the motor, τ is the motor parameter.

The preset acceleration and deceleration in the motor's braking phase are the same as those in the startup phase. Then the sliding speed $v_1(t)$ and $v_2(t)$ of the operating machinery during the braking phase can be expressed as eq. (17) and eq. (18).

$$v_1(t) = a\omega_1 r = a\omega_0 r \left(1 - e^{-t/\tau}\right) \tag{17}$$

$$v_2(t) = a\omega_2 r = a\omega_0 r \left(1 - e^{-(t-\Delta t)/\tau}\right) \tag{18}$$

where Δt is the acceleration and deceleration phase time in one cycle. a is a constant and is related to the structure of the object of research.

According to the Archard model, in a complete work cycle, when the contact stress p is a constant value, the calculation formulas for wear amount h_1, h_2, and h_3 in a starting phase, constant speed phase and braking phase are eq. (19), eq. (20), and eq. (21).

$$h_1 = \frac{k}{3\sigma_s \cos\lambda} \int_0^{t_1} p\omega_0 r \left(1 - e^{-t/\tau}\right) dt = m_1 p \tag{19}$$

$$h_2 = \frac{kv_0}{3\sigma_s \cos\lambda} \int_{t_1}^{t_2} p\, dt = m_2 p \tag{20}$$

$$h_3 = \frac{k}{3\sigma_s \cos\lambda} \int_{t_2}^{T} p\omega_0 r \left(1 - e^{(t-\Delta t)/\tau}\right) dt = m_3 p \tag{21}$$

B. TIME-VARYING WEAR MODEL

According to the Archard model, the wear process of running machinery is nonlinear in the starting and braking phases. Therefore, to accurately predict the wear of the worm gear tooth surface, it is necessary to consider the number of start and stop cycles experienced by the object of research. For mechanisms that frequently start and stop, the influence of contact stress on wear is significant. For different working methods, the contact stress needs to be updated frequently, and an iterative calculation process is needed to predict the object of research wear process. Considering that the wear of the worm gear is nonlinear, the working time is different and the wear process's calculation method is different. Therefore, under the condition of a specific working time t, the wear model of operating machinery varies under different conditions.

1) THE CONTACT STRESS P IS A FIXED VALUE

When the working condition of the object of research object is determined, the contact stress value can be determined according to the theoretical formula established by Hertz based on the elastic theory [41]. At this time, the contact stress can be regarded as a constant amount, and its specific amount is related to the determined working condition at different stages in a start-stop cycle. Refer to eq. (19), eq. (20), and eq. (21) to derive the amount of wear H(t), as shown at the bottom of the next page.

2) THE CONTACT STRESS P IS VARIABLE

When the operating machinery's actual working conditions are taken into consideration, the nominal contact stress calculated by the operating machinery may not be a constant amount value due to various reasons. The contact stress is affected by the specific mass of the load. The load of the research object is assumed to follow a normal distribution, then the nominal contact stress p is also a variable subject to the normal distribution.

$$p \sim N\left(\mu_{\mathrm{P}}, \sigma_{\mathrm{P}}^2\right) \tag{23}$$

where μ_{p} is the nominal contact stress. The contact stress p_1 is considered as a variable that obeys the normal distribution. For the convenience of expression, a piecewise function m(t) is introduced.

Combining the expression formulas of m_1, m_2, and m_3 in eq. (19), eq. (20), and eq. (21), the specific expression of the piecewise function $m(t)$ can be obtained. The expression of $m(t)$ is shown in eq. (25).

$$H(t) = p_1 \int \frac{kv\,(t)}{3\sigma_s} = p_1 m\,(t) \tag{24}$$

The difference between the function m(t) in eq. (25) and the h(t) in eq. (22), as shown at the bottom of the page is that the function $m(t)$ considers the contact stress p as a variable, so the change of p does not need to be considered separately in eq. (25), as shown at the bottom of the page.

3) ITERATIVE TIME-VARYING WEAR MODEL

When the operating machinery goes through $N+1$ cycles, in addition to the total amount of wear degradation H(t-NT) generated during the Nth cycle stage, it is also necessary to consider the iterative total of the previous N cycles of wear. According to the Archard model, the wear model for the first $N+1$ cycles is shown in eq. (26).

Among them, each cycle's wear amount in the first N cycles is related to the contact stress, and the uncertainty of the contact stress is considered. The eq. (26) can be further derived as eq. (27).

$$\begin{aligned} H(t) &= \sum_{n=1}^{N+1} h_n(t) \\ &= \sum_{n=1}^{N+1} h_n(v(n,t), p(n,t), \sigma_s, k) \\ &= \sum_{n=1}^{N+1} \int \frac{kp(n,t)v(n,t)}{3\sigma_s} dt \end{aligned} \tag{26}$$

where N is a natural number.

$$H(t) = n\,(h_1 + h_2 + h_3) + \sum_{j=1}^{N-n} (m_1 + m_2 + m_3)\,p_j + p_{N+1} m(t) \tag{27}$$

where n is the number of cycles in which the nominal contact stress experienced in the previous N cycles is a certain value p, and N-n is the number of cycles when the nominal contact stress p_i is an uncertain value.

IV. DCFP MODEL OF THE WORM GEAR IN THE HOIST

This paper uses a worm gear in a mine hoisting mechanism as the numerical case. A major advantage of choosing this primary research object is that the mine hoisting mechanism needs to start and stop frequently to achieve the work goal during work, so it must be considered that the sliding wear model of the operating mechanism is a nonlinear problem during the start and stop stage. Moreover, in the process of mine hoisting, the terminal load hoisting cycle consists of three stages: acceleration, constant speed, and deceleration [39]. The worm speed v_{worm} is divided into three stages, and the wear process needs to consider the influence of sliding speed. Another advantage of choosing this as the primary research object is that under different working conditions of the mine hoisting mechanism, the contact stress of the worm gear mechanism is uncertain due to the uncertainty of the working load. When the worm gear works normally, the contact stress p_{i} is a normal random variable and the contact

$$H(t) = h\,(t) = \begin{cases} a\dfrac{k}{3\sigma_s}\displaystyle\int_0^{t_1} p\omega_0 r\left(1 - e^{-t/\tau}\right) dt & 0 \le t < t_1 \\ h_1 + a\dfrac{kp_0\omega_0 r}{3\sigma_s}\displaystyle\int_{t_1}^{t} 1dt & t_1 \le t < t_2 \\ h_1 + h_2 + a\dfrac{kp_0\omega_0 r}{3\sigma_s}\displaystyle\int_{t_2}^{t}\left(1 - \exp\left(\dfrac{t-T}{\tau}\right)\right) dt & t_2 \le t < T \end{cases} \tag{22}$$

$$m(t) = \int \frac{kv\,(t)}{3\sigma_s} dt = \begin{cases} \dfrac{ak}{3\sigma_s}\displaystyle\int_0^{t} \omega_0 r\left(1 - e^{-\frac{t}{\tau}}\right) dt & 0 \le t < t_1 \\ m_1 + \dfrac{ak\omega_0 r}{3\sigma_s}\displaystyle\int_{t_1}^{t} 1dt & t_1 \le t < t_2 \\ m_1 + m_2 + \dfrac{ak\omega_0 r}{3\sigma_s}\displaystyle\int_{t_2}^{t}\left(1 - \exp\left((t-T)/\tau\right)\right) dt & t_2 \le t < T \end{cases} \tag{25}$$

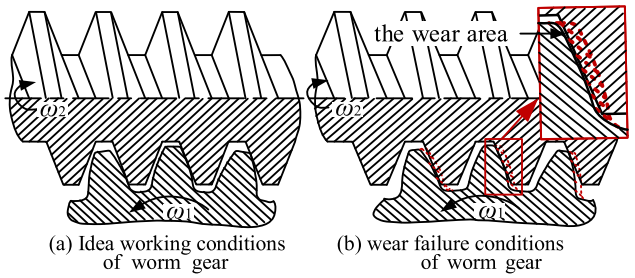

FIGURE 4. Failure mechanism diagram of a worm gear.

stress p_i is a constant value during a single lift. When the hoist is empty, the load of the empty car remains unchanged, so when the empty car drops the contact stress of the worm gear is a constant value p_0. The contact stress is a normal random variable p_i during the ith increase.

The focus of the degeneration modeling of the worm gear in the mine hoist is to analyze the sliding speed and contact stress of the worm gear. We chose the mine hoisting mechanism as the model's specific numerical case based on the particularity of its working nature.

A. DEPENDENCY ANALYSIS

In this section, we discuss the coupling relationship between worm gear wear degradation and random external shock, a topic on which there is a relatively small body of literature. When the worm mechanism is working, the worm wheel's wear will release worm wheel material particles into the gear oil, and correspondingly the worm will release steel particles. Worm gears are usually more prone to wear because they are made of a softer material than worms [42]. The worm gear wear failure mechanism diagram is shown in Fig. 4.

Under this working condition, the worm needs to overcome the backlash between the tooth profile of the worm and the tooth groove of the worm gear, which brings about a shock. This shock is considered to follow a random Poisson distribution. According to the extreme shock model, the random shock exceeding the hard failure threshold is regarded as a hard failure under the influence of random external shock. Besides, equipment wear degradation will reduce the mechanism's ability to withstand harmful shocks so that the hard failure threshold based on the extreme shock model decreases with the wear degradation process. We believe that the worm pair transmission's failure mode can be divided into two situations: (1) Soft failure caused by excessive wear of the worm gear. (2) When hoisting in a deep coal mine, due to the vibration of the hoisting system, the vertical rope length and the change of inertial load [43], [44] and the rolling of the rope on the rollers, the wire rope will slide back and forth [35].

For a better illustration, Fig. 5 shows the calculation process of the competitive failure reliability model in which wear degradation and random shock are interdependent. Then, the worm gear pair's reliability is obtained by analyzing the conditional probability of different situations.

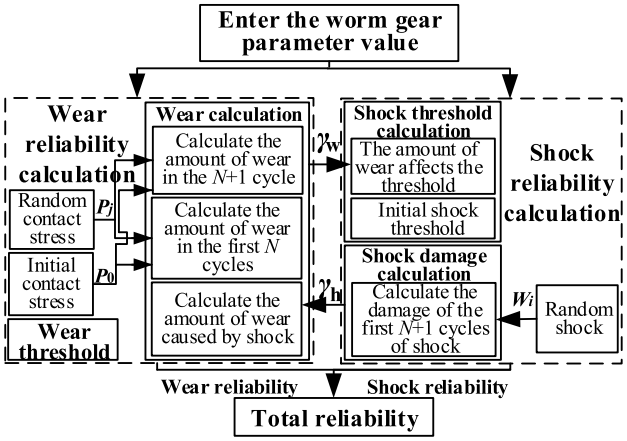

FIGURE 5. Reliability calculation flowchart.

1) THE HOIST IS IN THE FIRST DESCENDING STAGE (t<T)

When the mine hoisting mechanism is in the first descending stage, the working condition is that the empty car drops, the contact stress p is a constant, and the size is related to the quality of the empty car. Refer to eq. (27) to derive the wear amount $H(t)$.

(1) When i shocks occur at time t, the degradation reliability is shown in eq. (28), as shown at the bottom of next page.

(2) When i shocks occurs at time t, the shock reliability is shown in eq. (29), as shown at the bottom of the next page.

Then the total reliability at time t is shown in eq. (30), as shown at the bottom of the next page.

2) THE HOIST IS IN THE FIRST ASCENDING STAGE (T≤t<2T)

At this time, the surface contact stress p_1 is a random variable that follows the normal distribution $p \sim N(\mu_P, \sigma_P^2)$. Refer to eq. (19), eq. (20), and eq. (21), h_1, h_2 and h_3 are the amounts of wear in the starting, constant speed, and braking phases in a single cycle T. Combined with the eq. (27), the reliability formula under this working condition can be obtained.

(1) When i shocks occur at time t, the degradation reliability is shown in eq. (31), as shown at the bottom of the next page.

(2) When i shocks occurs at time t, the shock reliability of the i shocks is shown in eq. (32), as shown at the bottom of the next page. Then the total reliability at time t is shown in eq. (33), as shown at the bottom of the next page.

3) THE HOIST IS IN THE N + 1th DESCENDING STAGE (2NT ≤ t < (2N + 1)T)

Under this working condition, combined with eq. (27), the effect of the wear degradation process on the hard failure threshold needs to be considered.

(1) When i shocks occur at time t, the degradation reliability is shown in eq. (34), as shown at the bottom of page 50275.

(2) When i shocks occur at time t, the shock reliability of the i shocks is shown in eq. (35), as shown at the bottom of page 50275.

Then the total reliability at time t is shown in eq. (36), as shown at the bottom of the next page.

4) THE HOIST IS IN THE N + 1th ASCENDING STAGE ((2N + 1)T ≤ t < 2(N + 1)T)

When the total amount of wear degradation in the $N+1$th ascending phase has been calculated, it is necessary to consider the previous $N+1$ descending wear amount and the previous N ascending wear amount iterations $N+1$th ascending stage wear amount. The total amount of wear H(t) in this working stage is the same as the calculation method of the wear amount in the $N+1$th descent stage, and the influence of the contact stress P_{N+1} on the calculation of the wear degradation amount during the $N+1$th rise should be considered.

$$P\left(Z\left(t\right)<[Z]\left|N\left(t\right)=i\right.\right)P\left(N\left(t\right)=i\right)=P\left(H\left(t\right)+\gamma_h\sum_{j=1}^{i}W_j<[Z]\left|N\left(t\right)=i\right.\right)P\left(N\left(t\right)=i\right) \tag{28}$$

$$P\left(W_i<[W]\left|N\left(t\right)=i\right.\right)P\left(N\left(t\right)=i\right)=P\left(W_i<W_0+\gamma_w Z\left(t\right)\left|N\left(t\right)=i\right.\right)P\left(N\left(t\right)=i\right) \tag{29}$$

$$\begin{aligned}R\left(t\right)&=\sum_{i=1}^{\infty}P\left(Z\left(t\right)<[Z],W_i<[W]\left|N\left(t\right)=i\right.\right)P\left(N\left(t\right)=i\right)\\&=\sum_{i=1}^{\infty}P\left(\gamma_h\sum_{j=1}^{i}W_j<[Z]-h\left(t\right),W_i-\gamma_w\gamma_h\sum_{j=1}^{i-1}W_j<W_0+\gamma_w h\left(t\right)\left|N\left(t\right)=i\right.\right)\\&\quad\times P\left(N\left(t\right)=i\right)\\&=\sum_{i=1}^{\infty}\Phi\left(\frac{[Z]-h\left(t\right)-i\gamma_h\mu}{\sqrt{i\left(\gamma_h\sigma\right)^2}}\right)\Phi\left(\frac{W_0+\gamma_w h\left(t\right)-[1-(i-1)\gamma_w\gamma_h]\mu_w}{\sqrt{\sigma_w^2-(i-1)\left(\gamma_w\gamma_h\sigma_w\right)^2}}\right)\\&\quad\times\frac{\lambda\left(t\right)^i}{i!}\exp\left(-\lambda\left(t\right)\right)\end{aligned} \tag{30}$$

$$\begin{aligned}&P\left(Z\left(t\right)<[Z]\left|N\left(t\right)=i\right.\right)P\left(N\left(t\right)=i\right)\\&\quad=P\left(h\left(t\right)+\gamma_h\sum_{j=1}^{i}W_j<[Z]\left|N\left(t\right)=i\right.\right)P\left(N\left(t\right)=i\right)\\&\quad=P\left(h_1+h_2+h_3+p_1m\left(t-T\right)+\gamma_h\sum_{j=1}^{i}W_j<[Z]\left|N\left(t\right)=i\right.\right)P\left(N\left(t\right)=i\right)\end{aligned} \tag{31}$$

$$\begin{aligned}&P\left(W_i<[W]\left|N\left(t\right)=i\right.\right)P\left(N\left(t\right)=i\right)=P\left(W_i<W_0+\gamma_w Z\left(t\right)\left|N\left(t\right)=i\right.\right)P\left(N\left(t\right)=i\right)\\&\quad=P\left(W_i<W_0+\gamma_w\left[h_1+h_2+h_3+p_1m\left(t-T\right)+\gamma_h\sum_{j=1}^{i-1}W_j\right]\left|N\left(t\right)=i\right.\right)P\left(N\left(t\right)=i\right)\end{aligned} \tag{32}$$

$$\begin{aligned}R\left(t\right)&=\sum_{i=1}^{\infty}P\left(Z\left(t\right)<[Z],W_i<[W]\left|N\left(t\right)=i\right.\right)P\left(N\left(t\right)=i\right)\\&=\sum_{i=1}^{\infty}\left[P\left(p_1m\left(t-T\right)+\gamma_h\sum_{j=1}^{i}W_j<[Z]-\left(h_1+h_2+h_3\right),W_i-\gamma_w\gamma_h\sum_{j=1}^{i-1}W_j-\gamma_w p_1m\left(t-T\right)\right.\right.\\&\quad\left.\left.<\ W_0+\gamma_w\left(h_1+h_2+h_3\right)\left|N\left(t\right)=i\right.\right)\cdot P\left(N\left(t\right)=i\right)\right]\\&=\sum_{i=1}^{\infty}\left[\Phi\left(\frac{W_0+\gamma_w\left(h_1+h_2+h_3\right)-[1-(i-1)\gamma_w\gamma_h]\mu_w+\gamma_w m\left(t-T\right)t\mu_p}{\sqrt{\sigma_w^2-(i-1)\left(\gamma_w\gamma_h\sigma_w\right)^2-\left(\gamma_w m\left(t-T\right)\sigma_p\right)^2}}\right)\right.\\&\quad\left.\times\Phi\left(\frac{[Z]-\left(h_1+h_2+h_3\right)-m\left(t-T\right)\mu_p-i\gamma_h\mu_w}{\sqrt{m\left(t-T\right)\sigma_p^2+i\left(\gamma_h\sigma_w\right)^2}}\right)\cdot\frac{\lambda\left(t\right)^i}{i!}\exp\left(-\lambda\left(t\right)\right)\right]\end{aligned} \tag{33}$$

Under this working condition, combined with eq. (27), considering the coupling relationship between degradation and shock.

(1) When i shocks occur at time t, the degradation reliability is shown in eq. (37), as shown at the bottom of the page.

(2) When i shocks occur at time t, the shock reliability of the i shocks is shown in eq. (38), as shown at the bottom of the page.

Then the total reliability at time t is shown in eq. (39), as shown at the bottom of page 13.

$$
\begin{aligned}
&P\left(Z\left(t\right)<\left[Z\right]|N\left(t\right)=i\right)P\left(N\left(t\right)=i\right)\\
&=P\left(H\left(t\right)+\gamma_h\sum_{j=1}^{i}W_j<\left[Z\right]|N\left(t\right)=i\right)P\left(N\left(t\right)=i\right)\\
&=P\left(N\left(h_1+h_2+h_3\right)+\sum_{j=1}^{N}\left(m_1+m_2+m_3\right)p_j+h\left(t-NT\right)+\gamma_h\sum_{j=1}^{i}W_j<\left[Z\right]|N\left(t\right)=i\right)P\left(N\left(t\right)=i\right)
\end{aligned}
\tag{34}
$$

$$
\begin{aligned}
&P\left(W_i<\left[W\right]|N\left(t\right)=i\right)P\left(N\left(t\right)=i\right)\\
&=P\left(W_i<W_0+\gamma_wZ\left(t\right)|N\left(t\right)=i\right)P\left(N\left(t\right)=i\right)\\
&=P\left(W_i<W_0+\gamma_w\left[N\left(h_1+h_2+h_3\right)+\sum_{j=1}^{N}\left(m_1+m_2+m_3\right)p_j+h\left(t-NT\right)+\gamma_h\sum_{j=1}^{i-1}W_j\right]|N\left(t\right)=i\right)P\left(N\left(t\right)=i\right)
\end{aligned}
\tag{35}
$$

$$
\begin{aligned}
&R\left(t\right)=\sum_{i=1}^{\infty}P\left(Z\left(t\right)<\left[Z\right],W_i<\left[W\right]|N\left(t\right)=i\right)P\left(N\left(t\right)=i\right)\\
&=\sum_{i=1}^{\infty}\left[P\left(\sum_{j=1}^{N}\left(m_1+m_2+m_3\right)p_j+\gamma_h\sum_{j=1}^{i}W_j<\left[Z\right]-N\left(h_1+h_2+h_3\right)-h\left(t-NT\right),W_i-\gamma_w\gamma_h\sum_{j=1}^{i-1}W_j-\gamma_w\right.\right.\\
&\left.\left.\times\sum_{j=1}^{N}\left(m_1+m_2+m_3\right)p_j<W_0+\gamma_w\left[N\left(h_1+h_2+h_3\right)+h\left(t-NT\right)\right]|N\left(t\right)=i\right)P\left(N\left(t\right)=i\right)\right]\\
&=\sum_{i=1}^{\infty}\left[\Phi\left(\frac{\left[Z\right]-N\left(h_1+h_2+h_3\right)-h\left(t-NT\right)-N\left(m_1+m_2+m_3\right)\mu_p-i\gamma_h\mu_w}{\sqrt{N\left[\left(m_1+m_2+m_3\right)\sigma_p\right]^2+i\left(\gamma_h\sigma_w\right)^2}}\right)\cdot\right.\\
&\left.\Phi\left(\frac{W_0+\gamma_w\left[N\left(h_1+h_2+h_3\right)+h\left(t-NT\right)\right]-\left[1-\left(i-1\right)\gamma_w\gamma_h\right]\mu_w+N\gamma_w\left(m_1+m_2+m_3\right)\mu_p}{\sqrt{\sigma_w^2-\left(i-1\right)\left(\gamma_w\gamma_h\sigma_w\right)^2-N\left[\gamma_w\left(m_1+m_2+m_3\right)\sigma_p\right]^2}}\right)\frac{\lambda\left(t\right)^i}{i!}\exp\left(-\lambda\left(t\right)\right)\right]\\
&\times P\left(Z\left(t\right)<\left[Z\right]|N\left(t\right)=i\right)P\left(N\left(t\right)=i\right)
\end{aligned}
\tag{36}
$$

$$
\begin{aligned}
&=P\left(H\left(t\right)+\gamma_h\sum_{j=1}^{i}W_j<\left[Z\right]|N\left(t\right)=i\right)P\left(N\left(t\right)=i\right)\\
&=P\left(\left(N+1\right)\left(h_1+h_2+h_3\right)+\sum_{j=1}^{N}\left(m_1+m_2+m_3\right)p_j+p_{N+1}p_1m\left(t-NT\right)dt+\gamma_h\sum_{j=1}^{i}W_j<\left[Z\right]|N\left(t\right)=i\right)P\left(N\left(t\right)=i\right)
\end{aligned}
\tag{37}
$$

$$
\begin{aligned}
&P\left(W_i<\left[W\right]|N\left(t\right)=i\right)P\left(N\left(t\right)=i\right)\\
&=P\left(W_i<W_0+\gamma_wZ\left(t\right)|N\left(t\right)=i\right)P\left(N\left(t\right)=i\right)\\
&=P\left(W_i<W_0+\gamma_w\left[\left(N+1\right)\left(h_1+h_2+h_3\right)+\sum_{j=1}^{N}\left(m_1+m_2+m_3\right)p_j+p_{N+1}p_1m\left(t-NT\right)+\gamma_h\sum_{j=1}^{i-1}W_j\right]|N\left(t\right)=i\right)\\
&\times P\left(N\left(t\right)=i\right)
\end{aligned}
\tag{38}
$$

TABLE 1. Parameter values in the reliability Model.

Parameter	Value	Source
k	5×10^{-8}	Jbily et al. [6]
Z	1.8×10^{-2}	Jbily et al. [6]
T	30	assumption
t_1	5	assumption
W_0	1.5×10^{9}	Tanner et al. [49]
λ	5×10^{-5}	Jiang et al. [50]
γ_h	0.01Jia	assumption
γ_w	-10	assumption
μ	1×10^{8}	assumption
σ	3×10^{7}	assumption
μ_w	1.2×10^{9}	Rafiee et al. [21]
σ_w	0.2×10^{9}	Rafiee et al. [21]
P_0	2×10^{7}	assumption
ω_0	50	assumption
V_0	5	assumption
r	0.1	assumption
σ_s	$10^{9}/3$	Jbily et al. [6]
τ	2	assumption

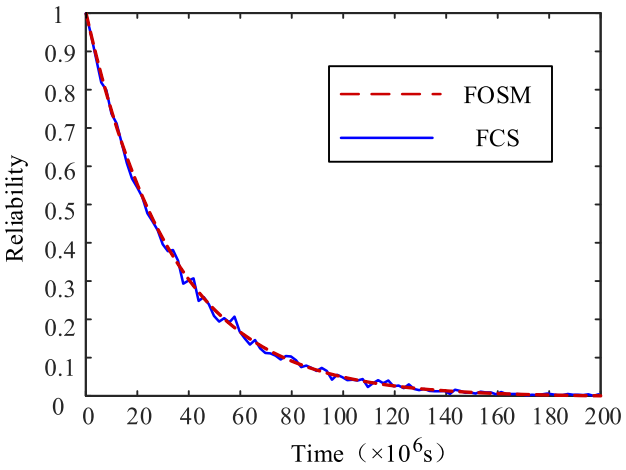

FIGURE 6. Comparison of the calculation results.

V. CASE STUDY

For the case study, we carried out a numerical example of a worm gear and worm drive mechanism made of tin bronze.

The material parameters involved in the model are shown in Table 1. We determined the worm gear wear threshold and the sliding wear rate of the worm gear material according to theoretical analysis of a wear model for worm gear in [5]. According to the given parameter values, the corresponding reliability curve is drawn in Fig. 6.

A. MONTE CARLO SIMULATION

In Section IV, in order to solve the time cost problem, we actually used the second-moment (FOSM) method to finally derive the reliability formula. In this section, we used a numerical method based on a Monte Carlo simulation (MCS) [46] to verify the accuracy of the algorithm. The MCS can be widely used in linear and nonlinear problems.

In order to ensure accuracy and consider the calculation efficiency at the same time, the selected sampling values are described below. The number of selected contact stress samples is 10^4, and the number of selected shock samples is 10^3.The calculated reliability curve with time is shown in Fig. 6. It can be seen that the reliability of the worm structure calculated by the FOSM and the MCS is roughly the same, which effectively verifies the accuracy of the reliability of the competitive failure model.

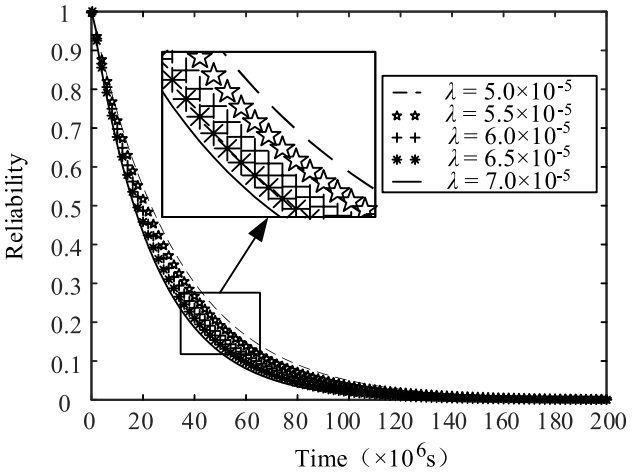

FIGURE 7. Reliability under different values of the dependence factor, λ.

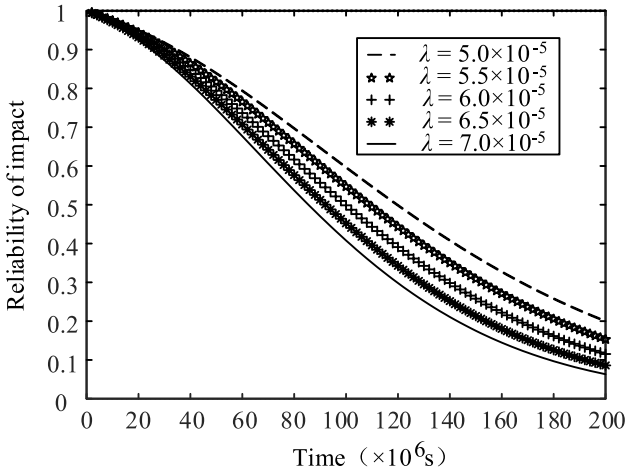

FIGURE 8. Shock reliability under different values of the dependence factor, λ.

B. PARAMETER COMPARISON OF RELIABILITY CURVES

Under the premise of ensuring that other parameters remain unchanged, we changed the Poisson shock rate λ to draw the degradation reliability, the shock reliability under different shock conditions, and the total reliability of the coupling of wear degradation and shock (39), as shown at the bottom of the next page.

In Fig. 7, it can be seen that in the initial working stage, the reliability of the worm drive mechanism gradually decreases,

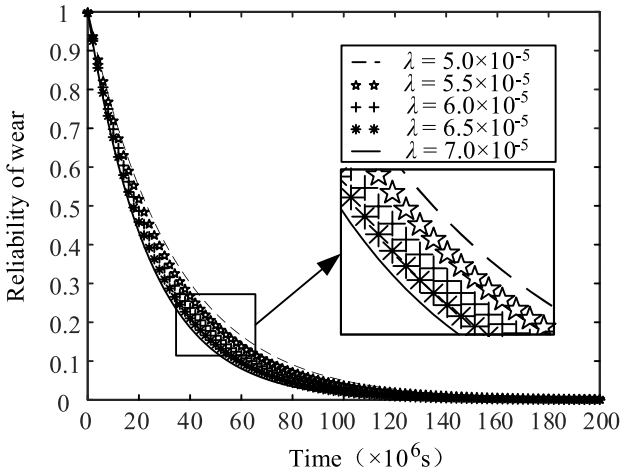

FIGURE 9. Wear reliability under different values of the dependence factor, λ.

and as time continues to increase, the worm drive mechanism completely fails.

The curve comparison chart is drawn in Fig. 7, Fig. 8, and Fig. 9. It can be seen that the three reliabilities will decrease with the increase of the Poisson shock rate λ. Worm failure is the result of the interaction of the wear degradation and the random external shock. From the separate calculations of the wear reliability and the shock reliability in Fig. 8 and Fig. 9, it can be seen that the reliability of wear is obviously lower than that of shock at the same time, so the life of the worm transmission mechanism in this case mainly depends on the wear degradation reliability.

C. SENSITIVITY ANALYSIS OF WEAR DEGRADATION PARAMETERS

In addition to the reliability analysis of the model with known parameters, in order to further determine the influence of the worm mechanism's working conditions on the wear degradation and soft failure, we calculate the average sensitivity of the shock and contact stress based on the first and second moments. In reliability analysis involving variable **X**, reliability is defined as

$$R = \Pr\{G = g(\mathrm{X}) \geq c\}$$

where Pr is the probability, G is the response, c is the limit state, $\mathrm{X} = (X_1, X_2, \ldots, X_i, \ldots, X_{nx})$ is the vector of random variables, the random function is called the performance function, also called the limit state function [47]. Performance functions can be used to calculate sensitivity [48]. The sum variance sensitivity is shown in Fig. 10, Fig. 11, and Fig. 12. We concluded that the external shock has a more significant effect on the wear degradation reliability of the worm drive, and that reducing the shock and the contact stress and reducing the variance of the two variables will increase the wear degradation reliability of the worm mechanism.

The calculated sensitivity of reliability to mean impact is shown in Fig.10. It can be seen that the sensitivity of reliability to the mean impact is negative. The reliability will decrease with the increase of the mean impact, and worm gear sets will tend to be unreliable (or fail). Moreover, the standard deviation of the impact have no obvious effect on the sensitivity of the reliability to the impact mean. With the increase of time, the sensitivity of reliability to mean impact first increase and then decrease. When the time is about 1.5×10^{8} s,

$$\begin{aligned}
R(t) &= \sum_{i=1}^{\infty} P(Z(t) < [Z], W_i < [W] \,|N(t) = i) P(N(t) = i) \\
&= \sum_{i=1}^{\infty} \Bigg[P\Bigg(\sum_{j=1}^{N} (m_1 + m_2 + m_3) p_j + p_{N+1} m(t - NT) + \gamma_h \sum_{j=1}^{i} W_j < [Z] - (N+1)\ (h_1 + h_2 + h_3), \\
&\quad \times W_i - \gamma_w \gamma_h \sum_{j=1}^{i-1} W_j - \gamma_w \sum_{j=1}^{N} (m_1 + m_2 + m_3) p_j - \gamma_w m(t - NT) p_{N+1} < W_0 + \gamma_w (N+1)(h_1 + h_2 + h_3) \\
&\quad \times |N(t) = i) \cdot P(N(t) = i)] \\
&= \sum_{i=1}^{\infty} \Bigg[\Phi\left(\frac{[Z] - (N+1) \sum_{i=1}^{3} h_i - \left[m(t - NT) + N \sum_{i=1}^{3} m_i \right] \mu_p - i \gamma_h \mu_w}{\sqrt{\left(m(t - NT)\sigma_p\right)^2 + N\left[(m_1 + m_2 + m_3)\sigma_p\right]^2 + i(\gamma_h \sigma_w)^2}} \right) \cdot \\
&\quad \cdot \Phi\left(\frac{W_0 + \gamma_w (N+1)(h_1 + h_2 + h_3) - [1 - (i-1)\gamma_w \gamma_h] \mu_w + \left[N \gamma_w (m_1 + m_2 + m_3) + \gamma_w m(t - NT) \right] \mu_p}{\sqrt{\sigma_w^2 - (i-1)(\gamma_w \gamma_h \sigma_w)^2 - N\left[\gamma_w (m_1 + m_2 + m_3)\sigma_p\right]^2 - \left(\gamma_w m(t - NT)\sigma_p\right)^2}} \right) \\
&\quad \times \frac{\lambda(t)^i}{i!} \exp(-\lambda(t)) \Bigg]
\end{aligned} \tag{39}$$

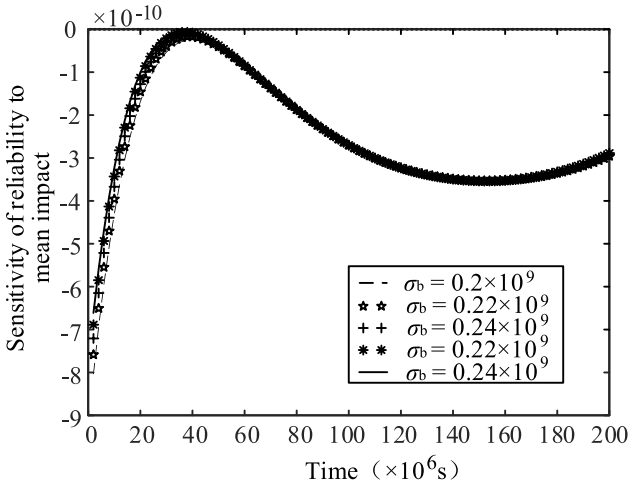

FIGURE 10. Sensitivity of reliability to mean shock under different values of the standard deviation of shock, σ_b.

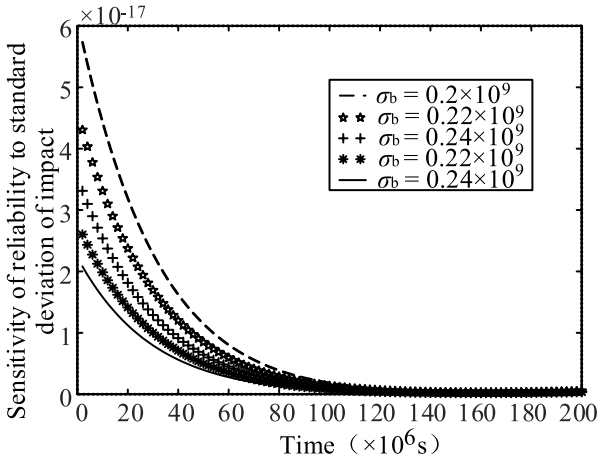

FIGURE 11. Sensitivity of reliability to standard deviation of shock under different values of the standard deviation of shock, σ_b.

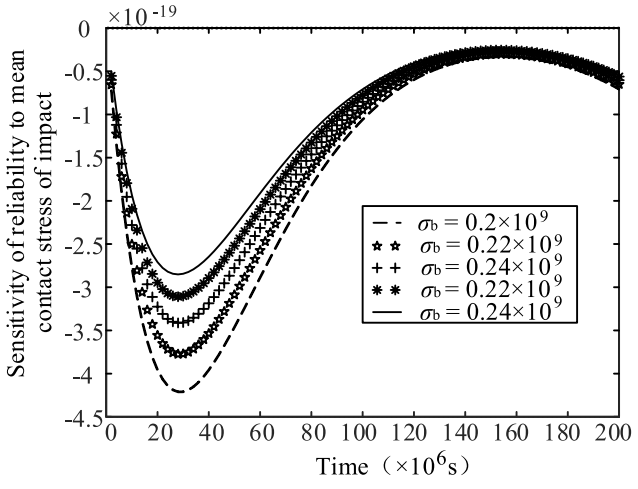

FIGURE 12. Sensitivity of reliability to mean contact stress of shock under different values of the standard deviation of shock, σ_b.

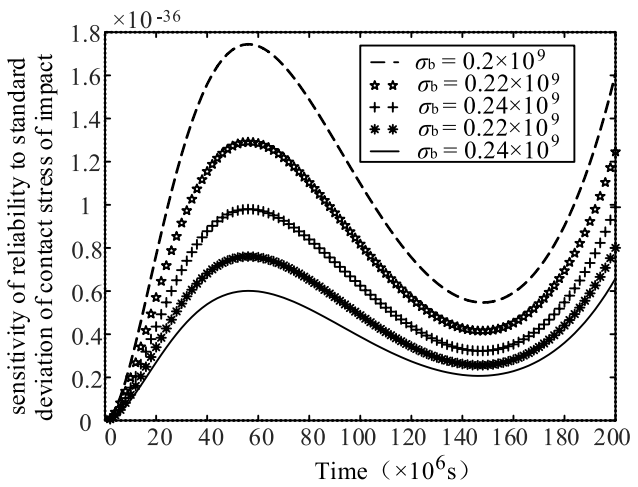

FIGURE 13. Sensitivity of reliability to standard deviation of contact stress of shock under different values of the standard deviation of shock, σ_b.

the value is the smallest, and the influence of the mean impact on the increase of the reliability is the minimum.

The calculated sensitivity of reliability to standard deviation of impact is shown in Fig.11. It shows that the sensitivity of reliability to the standard deviation of impact is positive, and the reliability will increase with the increase of the standard deviation of impact, and worm gear sets will tend to be more reliable. With the increase of time, the sensitivity of reliability to impact standard deviation becomes smaller and smaller, and the impact of impact standard deviation on the increase of reliability becomes smaller and smaller.

The calculated sensitivity of reliability to mean contact stress of impact is shown in Fig.12. It can be seen that the sensitivity of reliability to the mean contact stress is negative. When the contact stress increases, the reliability will decrease, and worm gear sets will tend to be unreliable (or fail). With the increase of impact standard deviation, the sensitivity of reliability to the mean value of contact stress becomes smaller and smaller, and the influence of the mean value of contact stress on the decrease of reliability becomes greater and greater. And it can also be concluded from Fig.12 that the sensitivity of the reliability to the mean contact stress doesn't change monotonically with time. When the time is about 1.5×10^8 s, the value is the smallest, and the influence of the mean contact stress on the decrease of the reliability is the largest.

The calculated sensitivity of reliability to standard deviation of contact stress of impact is shown in Fig.13. It can be seen that the sensitivity of reliability to the standard deviation of contact stress is positive, and with the increase of the standard deviation of contact stress, the reliability will increase and the worm gear set will tend to be more reliable. And with the increase of the impact standard deviation, the value of the sensitivity of reliability to the standard deviation of contact stress will also become larger and larger, which will have more and more influence on the increase of reliability. Moreover, it can be concluded from the figure that the value of the sensitivity of reliability to the standard deviation of contact stress doesn't change monotonically with time. When

the time is about 1.5×10^8 s, its value reaches the maximum and its influence on the increase of reliability is the greatest.

The calculation results show that the absolute value of the sensitivity of the reliability to the mean shock is the largest, and the shock on the change of the mean shock is the largest.

Therefore, in order to improve the reliability of the worm gear pair, certain measures can be taken to reduce the mean shock first.

VI. CONCLUSION

In this paper, we introduce a new reliability model that takes into account the relationship between wear degradation and random shock. The degradation conversion ratio coefficient represents the impact of the degradation process on the hard failure threshold, and the shock conversion ratio coefficient represents the impact of each harmful shock on the amount of wear degradation. Thereby, a competitive failure model of wear degradation and random shock of running machinery is established. This research realizes the replacement of the DCFP model with other simple mechanical structures except for micro-electromechanical systems. This research represents a new study of mechanical failure mechanisms and competitive failure processes. We selected the mine hoist's worm gear mechanism as a typical research object and verified the model. The two failure mechanisms of wear damage and shock failure will eventually lead to the worm gear reducer's failure, but these two failure mechanisms are interdependent. Through the establishment of a competitive failure model, it is found that the application of random shock will accelerate the progress of wear, and the reduction of the hard failure threshold is the result of gradual accumulation The resulting wear degradation process is a nonlinear model. Furthermore, comparing the calculation results with Monte Carlo simulation, it verifies that the calculation reliability of this method has certain accuracy. We used sensitivity calculation to discuss the influence of various parameters on reliability.

For the future investigation of this problem, additional-terms of dependence can be considered, such as the correlation between worm gear material, wear rate, and shock load, and the establishment of a degradation-shock coupling model related to the meshing number. It is also important to consider that the model's relevant parameters are known. In practical application, however, precise parameters may not be obtained. more correlations between soft failures and hard failures can be considered. For example, the shock process's impact on the increase in degradation can be extended from linear assumptions to nonlinear assumptions. The hypothesis that the shock obeys the Poisson distribution in this model can be extended to the non-Poisson distribution hypothesis, which will apply to more general situations. Last but not least, more shock models will be considered, including run shock models and δ shock models, and different definitions of harmful shocks will be proposed, which can be further studied in the future.

ACKNOWLEDGMENT

The authors would like to thank the reviewers and editors for their helpful comments on this article and the scientific research environment provided by CALCE.

REFERENCES

[1] R. Holm, *Electric Contacts*. Berlin, Germany: Springer, 1946, p. 214.
[2] J. F. Archard, "Contact and rubbing of flat surfaces," *J. Appl. Phys.*, vol. 24, no. 8, pp. 981–988, Aug. 1953.
[3] X.-S. Si, W. Wang, C.-H. Hu, D.-H. Zhou, and M. G. Pecht, "Remaining useful life estimation based on a nonlinear diffusion degradation process," *IEEE Trans. Rel.*, vol. 61, no. 1, pp. 50–67, Mar. 2012.
[4] K. J. Sharif, H. P. Evans, and R. W. Snidle, "Prediction of the wear pattern in worm gears," *Wear*, vol. 261, nos. 5–6, pp. 666–673, Sep. 2006.
[5] H. Ding and A. Kahraman, "Interactions between nonlinear spur gear dynamics and surface wear," *J. Sound Vibrat.*, vol. 307, nos. 3–5, pp. 662–679, Nov. 2007.
[6] D. Jbily, M. Guing, and J. P. De Vaujany, "A wear model for worm gear," *ARCHIVE Proc. Inst. Mech. Eng. C, J. Mech. Eng. Sci.*, vols. 203–210, pp. 1989–1996, Aug. 2015.
[7] F. A. Dorini and R. Sampaio, "Some results on the random wear coefficient of the archard model," *J. Appl. Mech.*, vol. 79, no. 5, pp. 3297–3308, Sep. 2012.
[8] V. Fontanari, M. Benedetti, G. Straffelini, C. Girardi, and L. Giordanino, "Tribological behavior of the bronze–steel pair for worm gearing," *Wear*, vol. 302, nos. 1–2, pp. 1520–1527, Apr. 2013.
[9] X. Wang and L. Morrish, "Predictions of wear and transmission errors of cylindrical worm gears," *Predictions Wear Transmiss. Errors Cylindrical Worm Gears*, vol. 4, pp. 869–874, Sep. 2003.
[10] L. Yuanyong, Z. Bo, and Q. Qingwen, "Analysis of the wear of gear transmission," in *Proc. EMEIT*, Harbin, China, Aug. 2011, pp. 4788–4790.
[11] D. Tang, J. Yu, X. Chen, and V. Makis, "An optimal condition-based maintenance policy for a degrading system subject to the competing risks of soft and hard failure," *Comput. Ind. Eng.*, vol. 83, pp. 100–110, May 2015.
[12] Y. Zhang, Y. Ma, L. Ouyang, and L. Liu, "A novel reliability model for multi-component systems subject to multiple dependent competing risks with degradation rate acceleration," *Eksploatacja i Niezawodnosc-Maintenance Rel.*, vol. 20, no. 4, pp. 579–589, Sep. 2018.
[13] H. Che, S. Zeng, J. Guo, and Y. Wang, "Reliability modeling for dependent competing failure processes with mutually dependent degradation process and shock process," *Rel. Eng. Syst. Saf.*, vol. 180, pp. 168–178, Dec. 2018.
[14] H. Gao, L. Cui, and Q. Qiu, "Reliability modeling for degradation-shock dependence systems with multiple species of shocks," *Rel. Eng. Syst. Saf.*, vol. 185, pp. 133–143, May 2019.
[15] Q. Qiu and L. Cui, "Gamma process based optimal mission abort policy," *Rel. Eng. Syst. Saf.*, vol. 190, Oct. 2019, pp. 106496.1–106496.9.
[16] S. Song, D. W. Coit, Q. Feng, and H. Peng, "Reliability analysis for multi-component systems subject to multiple dependent competing failure processes," *IEEE Trans. Rel.*, vol. 63, no. 1, pp. 334–345, Jan. 2014.
[17] Y.-H. Lin, Y.-F. Li, and E. Zio, "Reliability assessment of systems subject to dependent degradation processes and random shocks," *IIE Trans.*, vol. 48, no. 11, pp. 1072–1085, Aug. 2016.
[18] J. Wang, Q. Qiu, and H. Wang, "Joint optimization of condition-based and age-based replacement policy and inventory policy for a two-unit series system," *Rel. Eng. Syst. Saf.*, vol. 205, Jan. 2021, Art. no. 107251.
[19] J. J. Fan, S. G. Ghurye, and R. A. Levine, "Multicomponent lifetime distributions in the presence of ageing," *J. Appl. Probab.*, vol. 37, pp. 233–521, Jun. 2000.
[20] M. Fan, Z. Zeng, E. Zio, and R. Kang, "Modeling dependent competing failure processes with degradation-shock dependence," *Rel. Eng. Syst. Saf.*, vol. 165, pp. 422–430, Sep. 2017.
[21] K. Rafiee, Q. Feng, and D. W. Coit, "Reliability modeling for multiple dependent competing failure processes with changing degradation rate," *IIE Trans.*, vol. 46, pp. 196–483, Feb. 2014.
[22] A. Gut and J. Hüsler, "Realistic variation of shock models," *Statist. Probab. Lett.*, vol. 74, no. 2, pp. 187–204, Sep. 2005.
[23] N. Chatwattanasiri, D. W. Coit, N. Wattanapongsakorn, and Q. Feng, "Dynamic k-out-of-n system with component partnership design with two dependent competing failure processes," in *Proc. IEEE Int. Conf. Ind. Eng. Eng. Manage.*, Dec. 2013, pp. 1453–1457.

[24] Z. An and D. Sun, "Reliability modeling for systems subject to multiple dependent competing failure processes with shock loads above a certain level," *Rel. Eng. Syst. Saf.*, vol. 157, pp. 129–138, Jan. 2017.
[25] S. Hao and J. Yang, "Reliability analysis for dependent competing failure processes with changing degradation rate and hard failure threshold levels," *Comput. Ind. Eng.*, vol. 118, pp. 340–351, Apr. 2018.
[26] L. Jiang, Q. Feng, and D. W. Coit, "Reliability analysis for dependent failure processes and dependent failure threshold," in *Proc. ICQR2MSE*, Xi'an, China, Jun. 2011, pp. 30–34.
[27] H. Che, S. Zeng, and J. Guo, "A reliability model of micro-engines subject to natural degradation and dependent zoned shocks," *IEEE Access*, vol. 7, pp. 174951–174961, Dec. 2019.
[28] A. Lehmann, "Joint modeling of degradation and failure time data," *J. Stat. Planning Inference*, vol. 139, no. 5, pp. 1693–1706, May 2009.
[29] F. K. Choy, V. Polyshchuk, J. J. Zakrajsek, R. F. Handschuh, and D. P. Townsend, "Analysis of the effects of surface pitting and wear on the vibration of a gear transmission system," *Tribol. Int.*, vol. 29, no. 1, pp. 77–83, Feb. 1996.
[30] C. Yuksel and A. Kahraman, "Dynamic tooth loads of planetary gear sets having tooth profile wear," *Mechanism Mach. Theory*, vol. 39, no. 7, pp. 695–715, Jul. 2004.
[31] Y.-K. Gu, W.-F. Li, J. Zhang, and G.-Q. Qiu, "Effects of wear, backlash, and bearing clearance on dynamic characteristics of a spur gear system," *IEEE Access*, vol. 7, pp. 117639–117651, Aug. 2019.
[32] A. Flodin and S. Andersson, "Simulation of mild wear in spur gears," *Wear*, vol. 207, nos. 1–2, pp. 16–23, Jun. 1997.
[33] A. Kahraman, P. Bajpai, and N. E. Anderson, "Influence of tooth profile deviations on helical gear wear," *J. Mech. Design*, vol. 127, no. 4, pp. 656–663, Jul. 2005.
[34] M. Ognjanovic, "Progressive gear teeth wear and failure probability modeling," *Tribology Ind.*, vol. 26, pp. 44–49, Jan. 2004.
[35] H. Peng, Q. Feng, and D. W. Coit, "Reliability and maintenance modeling for systems subject to multiple dependent competing failure processes," *IIE Trans.*, vol. 43, no. 1, pp. 12–22, Oct. 2010.
[36] S. Mathew, D. Das, R. Rossenberger, and M. Pecht, "Failure mechanisms based prognostics," in *Proc. PHM*, Denver, CO, USA, 2008, pp. 1–6.
[37] G. J. Dolecek, "Normal random variable," in *Random Signals Processes Primer With MATLAB*. New York, NY, USA: Springer, 2013, pp. 227–229.
[38] R. L. Deuis, C. Subramanian, and J. M. Yellup, "Dry sliding wear of aluminium composites—A review," *Compos. Sci. Technol.*, vol. 57, pp. 415–435, Oct. 1997.
[39] D. Wang, D. Zhang, Z. Zhang, and S. Ge, "Effect of various kinematic parameters of mine hoist on fretting parameters of hoisting rope and a new fretting fatigue test apparatus of steel wires," *Eng. Failure Anal.*, vol. 22, pp. 92–112, Jun. 2012.
[40] Z. S. Yang and X. M. Ma, "Synthesis of mine hoist speed curve based on programmable logic controller," *Adv. Mater. Res.*, vols. 846–847, pp. 90–93, Nov. 2013.
[41] G. FitzGerald, "Hertz's miscellaneous papers," *Nature*, vol. 55, pp. 6–9, Nov. 1896.
[42] V. Pekka, S. Lahdelma, and J. Leinonen, "On the condition monitoring of worm gears," in *Proc. WCEAM*, London, U.K., 2006, pp. 332–343.
[43] D. Wang, D. Zhang, and S. Ge, "Effect of terminal mass on fretting and fatigue parameters of a hoisting rope during a lifting cycle in coal mine," *Eng. Failure Anal.*, vol. 36, pp. 404–422, Jan. 2014.
[44] D. Wang, X. Li, X. Wang, G. Shi, X. Mao, and D. Wang, "Effects of hoisting parameters on dynamic contact characteristics between the rope and friction lining in a deep coal mine," *Tribol. Int.*, vol. 96, pp. 12–34, Apr. 2016.
[45] X.-D. Chang, Y.-X. Peng, Z.-C. Zhu, X.-S. Gong, Z.-F. Yu, Z.-T. Mi, and C.-M. Xu, "Effects of strand lay direction and crossing angle on tribological behavior of winding hoist rope," *Materials*, vol. 10, no. 6, p. 630, Jun. 2017.
[46] R. L. Wasserstein, "Monte Carlo: Concepts, algorithms, and applications," *Technometrics*, vol. 39, p. 338, Aug. 1997.
[47] S. Mahadevan, "Physics-based reliability mode," in *Reliability-based Mechanical Design*. New York, NY, USA: Dekker, 1997.
[48] J. Guo and X. Du, "Reliability sensitivity analysis with random and interval variables," *Int. J. Numer. Methods Eng.*, vol. 78, no. 13, pp. 1585–1617, Jun. 2009.
[49] D. M. Tanner and M. T. Dugger, "Wear mechanisms in a reliability methodology," *Proc. SPIE*, vol. 4980, pp. 22–40, Feb. 2003.
[50] L. Jiang, Q. Feng, and D. W. Coit, "Reliability and maintenance modeling for dependent competing failure processes with shifting failure thresholds," *IEEE Trans. Rel.*, vol. 61, no. 4, pp. 932–948, Dec. 2012.

HAO LYU was born in China, in 1982. He received the B.S. and M.S. degrees from the School of Automobile, Chang'an University, China, in 2010, and the Ph.D. degree in mechanical engineering from Northeastern University, China, in 2014. Since 2014, he has been a Lecturer with Northeastern University. Since 2020, he has also been a Visiting Scholar with the CALCE, University of Maryland. He is the author of one book, more than ten articles, and more than ten inventions. His research interests include calculation method of reliability, mechanical reliability, dynamic reliability, mechanical vibration, and vehicle reliability.

XIAOWEN ZHANG was born in China, in 1997. She received the bachelor's degree in mechanical engineering from Northeastern University, China, in 2015. She is currently pursuing the Ph.D. degree with Northeastern University. Her research interests include mechanical reliability design, reliability calculation methods, and reliability modeling and design.

ZAIYOU YANG received the M.S. degree in mechanical engineering from the Guangxi University of Science and Technology, Liuzhou, Guangxi, in 2017. He is currently pursuing the Ph.D. degree in mechanical engineering with Northeast University, Shenyang, Liaoning, China. His research interests include reliability modeling and simulation, reliability analysis, and optimization.

SHUAI WANG, photograph and biography not available at the time of publication.

CHANGYOU LI, photograph and biography not available at the time of publication.

MICHAEL PECHT (Life Fellow, IEEE) received the B.S. degree in acoustics, the M.S. degree in electrical engineering, and the M.S. and Ph.D. degrees in engineering mechanics from the University of Wisconsin at Madison. He is currently a Professional Engineer, and an ASME Fellow. He received the 3M Research Award for electronics packaging, the IEEE Undergraduate Teaching Award, and the IMAPS William D. Ashman Memorial Achievement Award for his contributions in electronics reliability analysis. He has written 18 books on electronic products development, use, and supply chain management. He is also the Chief Editor of *Microelectronics Reliability* and an Associate Editor of the IEEE TRANSACTIONS ON COMPONENTS AND PACKAGING TECHNOLOGY. He is also the Founder of the Center for Advanced Life Cycle Engineering (CALCE) and the Electronic Products and Systems Consortium, University of Maryland.